Static magnetization and ac susceptibility measurements of the copper-oxygen cluster compound $BaCuO_{2+x}$

Z. R. Wang, D. C. Johnston, L. L. Miller, and D. Vaknin
Ames Laboratory and Department of Physics and Astronomy, Iowa State University, Ames, Iowa 50011
(Received 26 April 1995; revised manuscript received 30 May 1995)

Static magnetization M and ac magnetic susceptibility measurements in applied magnetic fields H up to 55 kG are reported for a polycrystalline He-annealed sample of $BaCuO_{2+x}$ with $x = 0.1 \pm 0.1$. This compound has a large body-centered-cubic unit cell ($a_0 = 18.29$ Å) containing 90 formula units. The cell contains six lone CuO_4 units, two $Cu_{18}O_{24}$ sphere clusters, and eight Cu_6O_{12} ring clusters. Clear evidence of long-range antiferromagnetic (AF) ordering at a Néel temperature $T_N \sim 15$ K was found. From detailed analyses of isothermal $M(H)$ data at 2 K and static magnetic susceptibility data from 2 to 400 K, the following model for the magnetic properties of $BaCuO_{2+x}$ emerged. The oxidation state of the copper is +2, and each Cu^{+2} ion carries a spin $S_{Cu} = 1/2$. The Cu_{18} sphere clusters and Cu_6 ring clusters both have ferromagnetic ground states with spins $S_s = 9$ and $S_r = 3$, respectively, with lower spin excited states. The ferromagnetic intracluster interactions arise from a Cu-O-Cu superexchange pathway with a nearly 90° bond angle; within the sphere and ring clusters, the Cu-Cu superexchange coupling constants are $2J_s/k_B = (80 \pm 16)$ K and $2J_r/k_B = (290 \pm 60)$ K, respectively. The clusters are in their ground states below ~ 40 K. The AF ordering at T_N arises from AF ordering of the Cu_6 spin 3 magnetic moments only; this aspect of our model has been confirmed by magnetic neutron-diffraction measurements. Remarkably, the Cu_{18} clusters and lone Cu ions do not participate in this ordering and remain paramagnetic down to at least 2 K. Each Cu_{18} cluster is antiferromagnetically coupled to three lone Cu ions, and each lone Cu ion to one Cu_{18} cluster, with AF coupling constant $2J_{AF}/k_B = -0.33$ K. The Cu_{18} clusters (with spin $S_s = 9$) are predicted to undergo ferromagnetic intercluster ordering below ~ 1 K.

I. INTRODUCTION

The structures of all known high-transition temperature T_c cuprate superconductors contain CuO_2 planes.[1] The parent (undoped) insulator (at $T = 0$) phases of those materials exhibit long-range antiferromagnetic (AF) ordering of the Cu^{+2} (d^9) magnetic moments below a Néel temperature $T_N < 550$ K,[2,3] and dynamic two-dimensional AF short-range ordering above T_N.[4,5] Furthermore, upon doping, the insulating parent materials become metallic and T_N drops to zero, but short-range AF order survives within the CuO_2 planes.[3–6] The short-range AF order may play an important role in the mechanism of the high-temperature superconductivity.[7] The strong AF interaction ($2J \sim -1500$ K) between the Cu spins in the CuO_2 planes[3,5] originates from the indirect 180°-bond-angle Cu^{+2}-O^{-2}-Cu^{+2} superexchange interaction.[8,9] Aharony *et al.*[10] and others[11] have argued that an intervening O^{-1} ion produced by a localized doped hole on the O^{-2} ion results instead in an indirect *ferromagnetic* (FM) interaction between the two adjacent Cu spins. This FM interaction would result in magnetic frustration, which may be relevant to the superconducting pairing mechanism in the high-T_c cuprates.[10] However, an alternative cause of FM interactions has been predicted[9] to be a change in the Cu^{+2}-O^{-2}-Cu^{+2} bond angle from 180° to 90°. This bond angle has recently been inferred by Büchner *et al.*[12] to be important to the occurrence of superconductivity. Their experiments showed that when the tilt angle of the CuO_6 octahedra in $La_{2-x-y}Sr_xNd_yCuO_4$ decreases below 3.6°, i.e., as the Cu-O-Cu bond angle approaches 180°, the superconductivity is destroyed. Thus it is important to further clarify the conditions under which FM versus AF Cu^{+2}-Cu^{+2} interactions occur in copper oxides.

A FM Cu^{+2}-Cu^{+2} interaction has been found in several copper oxide compounds. For example, in $La_4Ba_2Cu_2O_{10}$ a bulk three-dimensional FM transition at 5.2 K was detected.[13] The structure of this compound contains isolated square-planar CuO_4 units. The planes of adjacent CuO_4 units are nearly perpendicular to each other. The Cu-O-Cu bond angle is 114.2°, and the respective Cu-O and O-Cu distances are 1.82 Å and 3.80 Å. Since the latter distance is much larger than the sum of the Cu^{+2} and O^{-2} ionic radii, the FM Cu-Cu coupling is very weak ($J = 2.6$ K).[13] Another example is Li_2CuO_2,[14,15] in which square-planar CuO_4 units are edge shared to form infinite chains. The intrachain Cu^{+2}-O^{-2}-Cu^{+2} bond angle is 94.0°, and the Cu^{+2}-O^{-2} distance is 1.96 Å.[14] Specific heat and magnetic susceptibility measurements show an AF ordering transition at $T_N = 9.3$ K.[16] However, neutron-diffraction measurements revealed that, below T_N, the spins in the chains are ferromagnetically aligned as expected from the Cu^{+2}-O^{-2}-Cu^{+2} bond angle, and the AF character below T_N arises from AF alignment of the spins in adjacent chains.[14,17]

The material studied in this work is $BaCuO_{2+x}$. When $x \sim 0$, this compound has a large body-centered-cubic

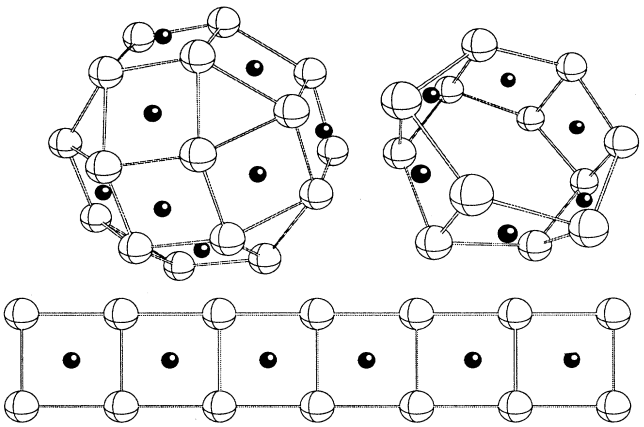

FIG. 1. Perspective representation of the two types of Cu-O clusters in the bcc unit cell of $BaCuO_{2+x}$. The $Cu_{18}O_{24}$ sphere clusters (upper left) are located at the (0,0,0) position and at the (1/2,1/2,1/2) position. The Cu_6O_{12} ring clusters (upper right) are located at the (1/4,1/4,1/4) position and at the remaining seven equivalent positions with their axis of highest symmetry along the corresponding body diagonal. Lone Cu ions are located on the edges of the unit cell between the sphere clusters (statistically one-half occupied). Both clusters consist of closed one-dimensional strips of edge-sharing square pyrimidal CuO_4 units. An unrolled strip of such one-dimensional edge-sharing CuO_4 squares is shown at the bottom.

unit cell ($a_0 = 18.277$ Å) with 90 formula units/cell.[18,19] As illustrated in Fig. 1 of Ref. 20, the cell contains six lone CuO_4 units, eight Cu_6O_{12} ring clusters, and two $Cu_{18}O_{24}$ sphere clusters. A picture of the clusters is shown in Fig. 1. Within the ring clusters, the Cu-O-Cu bond angle is 82.83°, the Cu-O distance is 1.969 Å, and the Cu-Cu distance is 2.605 Å, whereas within the sphere clusters, the Cu-O-Cu bond angle is 86.86°, the Cu-O distance is 1.98 Å, and the Cu–Cu distance is 2.698 Å.[19] A picture of an unfolded ring is shown in Fig. 1. Because these bond angles are rather close to 90°, one would expect the Cu spins in the Cu_6 and Cu_{18} clusters to be ferromagnetically coupled.

By considering the atomic position occupancies of $BaCuO_{2+x}$ from the structure determined using single-crystal x-ray diffraction, Kipka and Müller-Buschbaum[18] obtained the composition $BaCuO_2$. Similarly, Weller and Lines[19] found the compositions of two samples to be $BaCuO_2$ and $BaCuO_{2.07}$. They also measured the oxygen content of a sample by thermogravimetric analysis (TGA) to be $BaCuO_{2.08\pm0.02}$. From structural analysis on a single crystal, Paulus *et al.*[21] found the oxygen content to be 2.28 by modifying the crystal model obtained by Kipka and Müller-Buschbaum.[18] Using iodometric titration, Eriksson *et al.*[22] found the oxygen content to be between 1.8 and 2.05. Therefore the oxygen content of $BaCuO_{2+x}$ appears to be variable.[23] Recently, Aranda and Attfield[24] reported simultaneous refinements of x-ray and neutron powder-diffraction patterns of $BaCuO_{2+x}$, indicating that carbonate ions (CO_3^{-2}) are included within the unit cell. They proposed that the carbonate ions are essential for stabilizing the clusterlike structure described above and that the chemical formula of the compound should be $Ba_{44}Cu_{48}(CO_3)_6O_{81+x}$ [with $x = 6.9(3)$ for their sample]. According to Aranda and Attfield, the carbonate ions are located outside the Cu-O clusters, and therefore may play some role in the magnetic coupling between clusters, but not within the clusters. In this paper, their role will not be explicitly considered.

Specific-heat measurements have been reported by Eckert *et al.*[25] The results vary from sample to sample below ~ 15 K. For a sample prepared in air, a (magnetic) phase transition was found at about 13 K.

Electrical conductivity σ measurements have been reported by Migeon *et al.*[26] The conductivity was found to be activated, with an activation energy of 0.61 eV for $BaCuO_2$, but which decreased with increasing oxygen content. A slope change was found in $\ln(\sigma)$ versus $1/T$ at ≈ 370 K,[27] for both $BaCuO_2$ (cubic) and $BaCuO_{2.5}$ (orthorhombic) samples.

The magnetic properties of $BaCuO_{2+x}$ have been previously measured by several research groups. From electron spin resonance (ESR) measurements, Vier *et al.*[28] and de Mesquita *et al.*[29] concluded that the resonance observed at room temperature originated from Cu^{2+} ($3d^9$). Vier *et al.* found the peak-to-peak linewidth to have a minimum at about 15 K, which can be associated with a magnetic phase transition, but the magnetic structure was unknown. They also found that the static magnetic susceptibility χ versus temperature T can be characterized by different behaviors in two different temperature ranges. For $T > 100$ K, the $1/\chi$-versus-temperature plot shows a linear (Curie-Weiss) behavior, which corresponds to an effective magnetic moment $\mu_{\rm eff}$ of $1.72\mu_B$ per Cu ion; at lower temperatures, the $1/\chi$-versus-T curve shows positive curvature and $\mu_{\rm eff}$ increases, reaching a value of $3.16\mu_B$ below 30 K. Recently Petricek, Bukovec, and Bukovec[30] reported the observation of an antiferromagnetic to diamagnetic transition at about 3 K from $\chi(T)$ measurements for their sample of $BaCuO_{2.5}$ (with a noncubic structure).

Here, we report static magnetization M and magnetic susceptibility χ, and ac magnetic susceptibility measurements of $BaCuO_{2+x}$ with $x = 0.1 \pm 0.1$ from 2 to 400 K in magnetic fields H up to 55 kG. Our study was initially motivated by the observation of an anomalously strong, crystallographically forbidden (111) peak in the neutron-diffraction pattern of this compound at 4 K, which was not present at 300 K.[31] These observations suggested that this reflection was magnetic in origin.[31] On the other hand, the intensity of this peak was comparable to those of adjacent structural peaks, and the various magnetic structures modeled could not explain the intensity of this peak and the simultaneous absence of other magnetic peaks. We successfully resolved the nature of and provided a model for the magnetic structure of the magnetic phase below 15 K via analysis of $M(H,T)$ and $\chi(T)$ measurements.[20] This model has been verified by subsequent polarized and unpolarized magnetic neutron-diffraction measurements.[20,32] In Ref. 20, only an outline of some of our results and analyses was

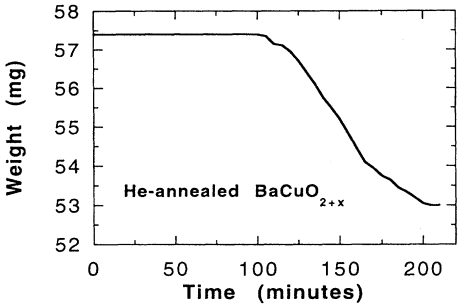

FIG. 2. Thermogravimeteric analysis (TGA) data for He-annealed $BaCuO_{2+x}$. The data were taken in 5% H_2/He at a rate of 5 °C/min up to 950 °C and then kept at 950 °C for 30 min.

given. Here, we present more extensive $M(H,T)$ data up to 300 K and describe in more detail the analysis of the low-T data. Also, ac susceptibility data for $T < 50$ K are presented, which clearly reveal the AF transition at ~ 15 K. In addition, we present an analysis of the $\chi(T)$ data from 70 to 400 K, which has now allowed us to extract the FM Cu-Cu intracluster superexchange interaction constants. Following the experimental details in Sec. II, we present our $M(H,T)$ and ac susceptibility data in Sec. III, where preliminary analyses are also given. The detailed analyses of the low-temperature ($T \ll T_N$) $M(H,$ 2 K) and $\chi(T)$ data, of the high-temperature ($T > 70$ K) $\chi(T)$ data, and our resulting model for the magnetism of $BaCuO_{2+x}$, are presented in Sec. IV. We conclude with a summary and discussion of the results in Sec. V.

II. EXPERIMENTAL DETAILS

The synthesis of our He-annealed $BaCuO_{2+x}$ sample is described in Ref. 20. The oxygen content of this sample was measured using TGA, as shown in Fig. 2. From the weight loss, we calculated the (initial) oxygen content of the sample to be 2.1 ± 0.1.

Powder x-ray-diffraction measurements were carried out using a Rigaku diffractometer, with a curved graphite crystal monochromator, using Cu $K\alpha$ radiation. The x-ray pattern for the sample is shown in Fig. 3. The peaks were indexed according to the structural model obtained by Kipka and Müller-Buschbaum[18] and Weller and Lines,[19] and no impurity peaks were found. The peak positions were corrected for zero-point shift and nonlinearity using Si as an internal standard. The lattice parameter a_0 was obtained using the least-squares fitting program FINAX, yielding $a_0 = 18.29 \pm 0.03$ Å. This value is the same within the errors as values obtained by Weller and Lines (18.277 – 18.286 Å),[19] Migeon *et al.* (18.28 – 18.31 Å),[26] and Eriksson *et al.* (18.27 – 18.32 Å).[22,23] The structure of our sample was found from neutron-diffraction measurements[33] to be essentially the same as that previously proposed in Refs. 18 and 19.

ac magnetic susceptibility measurements were made on a Lake Shore ACS7000 ac susceptometer. The amplitude of the ac field was kept at 100 G and the frequency at 125 Hz. The measurements versus T were performed under constant H in the range of 0 – 55 kG. $M(H,T)$ data were obtained using a Quantum Design superconducting quantum interference device (SQUID) magnetometer.

III. EXPERIMENTAL RESULTS AND PRELIMINARY ANALYSIS

The observed χ of $BaCuO_{2+x}$ is expected to be the sum of three terms: $\chi = \chi^{dia} + \chi^{VV} + \chi^{spin}$, where the first term is due to the orbital diamagnetism of the closed electron shells of the atoms, the second is the paramagnetic orbital Van Vleck susceptibility of the Cu^{+2} ions and the third term is the spin susceptibility of the Cu^{+2} ions. From standard tables,[34] one obtains $\chi^{dia} = -6.8 \times 10^{-5}$ cm^3/mol for $BaCuO_2$ and $\chi^{dia} = -7.4 \times 10^{-5}$ cm^3/mol for $BaCuO_{2.5}$. The anisotropic χ^{VV} values for Cu^{+2} in the layered high-T_c cuprates have been estimated in, for example, Ref. 35. For our samples, we take the powder average of those values and estimate that $\chi^{VV} \approx 7.4 \times 10^{-5}$ cm^3/mol.

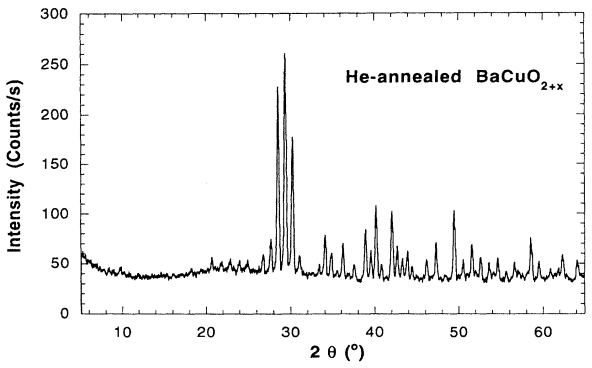

FIG. 3. Powder x-ray-diffraction pattern for He-annealed $BaCuO_{2+x}$, obtained using Cu$K\alpha$ radiation.

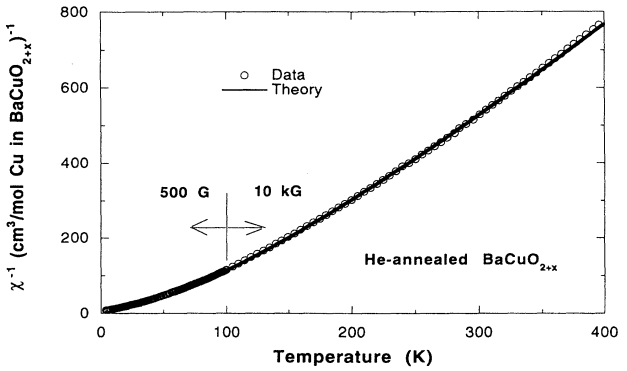

FIG. 4. Inverse magnetic susceptibility χ^{-1} vs temperature for He-annealed $BaCuO_{2+x}$ (circles). The solid curve is a theoretical fit [Eqs. (18) and (19)] to the data above 70 K.

Thus, the sum $\chi^{\rm dia}+\chi^{\rm VV}$ is nearly zero, and we will neglect it. Also, since $\chi \simeq \chi^{\rm spin}$, we will henceforth denote $\chi^{\rm spin}$ by χ to simplify notation.

Shown in Fig. 4 is the inverse molar magnetic susceptibility χ^{-1} versus T of our He-annealed sample of $BaCuO_{2+x}$.[20] At high-T ($\geq$ 300 K), $\chi^{-1}(T)$ increases linearly with temperature (Curie-Weiss law):

$$\chi^{-1} = (T-\theta)/C\,, \tag{1}$$

where

$$C = N_A g^2 S(S+1)\mu_B^2/3k_B = N_A \mu_{\rm eff}^2/3k_B \tag{2}$$

is the molar Curie constant, N_A is Avogadro's number, g and S are, respectively, the gyromagnetic factor and the spin of the paramagnetic species, μ_B is the Bohr magneton and k_B is Boltzmann's constant. By fitting Eq. (1) to the data in the temperature range between 300 and 400 K, one gets C = 0.39 cm^3 K/mol Cu, g = 2.10 $\pm$ 0.04 (assuming the spin of a Cu^{+2} ion is $S_{\rm Cu}$= 1/2), θ = 81 K, and $\mu_{\rm eff}$ = 1.82μ_B/Cu atom.[20] The g value is similar to the powder average ($g = [(g_x^2+g_y^2+g_z^2)/3]^{1/2}$ = 2.15) of the values (g_x = 2.27, g_y = 2.12, g_z = 2.05) obtained from the ESR measurements.[28] Thus, at high-T, He-annealed $BaCuO_{2+x}$ behaves as if all Cu^{+2} spins are equivalent spins 1/2 interacting ferromagnetically.

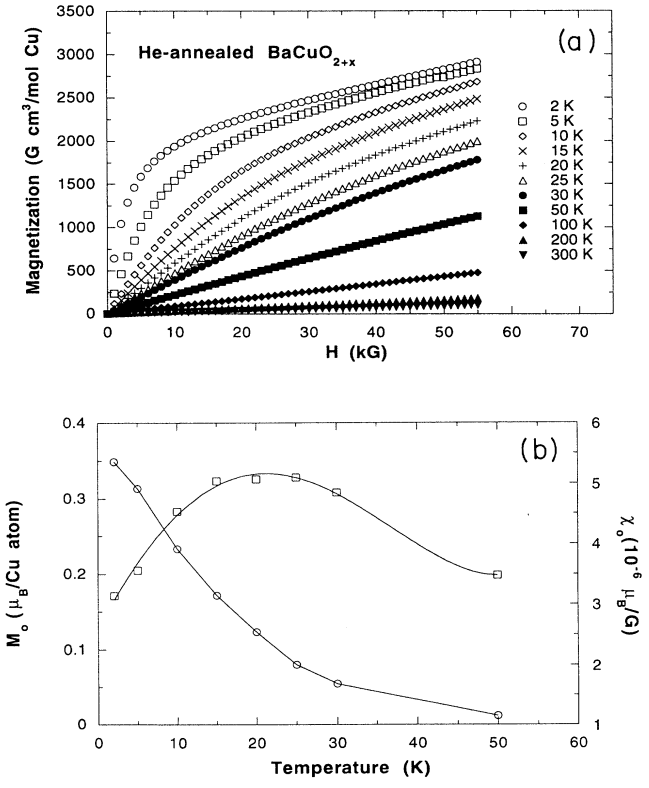

FIG. 5. (a) Magnetization vs applied magnetic field H at various indicated temperatures for He-annealed $BaCuO_{2+x}$. (b) Slope χ_0 (squares, right-hand scale) and y-intercept M_0 (circles, left-hand scale) of straight-line fits to the data in (a) between 30 and 55 kG. The solid curves are guides to the eye.

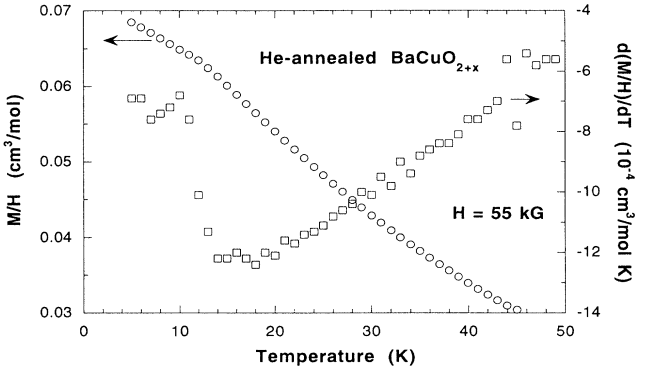

FIG. 6. High-field (H = 55 kG) magnetization M divided by H vs temperature for He-annealed $BaCuO_{2+x}$ (circles). The temperature derivative of these data computed from adjacent data points vs temperature (squares) is also shown.

However, contrary to the prediction[36] of molecular field theory, (long-range) FM order is not observed at (or below) $T = \theta$ = 81 K. Rather, χ^{-1} exhibits positive curvature with decreasing T and then eventually exhibits linear Curie-Weiss behavior again between 2 and 6 K, with C = 1.13 cm^3 K/mol Cu, θ = 0.4 K, and $\mu_{\rm eff}$ = 3.01μ_B/Cu atom.[20] The FM sign of θ and the large increase of C with decreasing T suggests that the Cu_{18} and Cu_6 clusters in $BaCuO_{2+x}$ have maximal spin 9 and spin 3 ground states and spin 8,7, ..., 0 and spin 2,1,0 excited states, respectively. Indeed, the shape of $\chi^{-1}(T)$ in Fig. 4 is very similar to that of a $(Cr^{+3})_4$ cluster with a maximal spin 6 ground state and spin 5,4, ..., 0 excited states.[37]

In order to further clarify the magnetic character of $BaCuO_{2+x}$, $M(H)$ isotherms were obtained at various temperatures between 2 and 300 K, as shown in Fig. 5(a). With decreasing temperature below $\sim$ 50 K, the $M(H)$ data exhibit increasingly pronounced negative curvature. The slope of the data χ_0 at the highest fields (30–55 kG) exhibits a peak at a temperature between 15 and 25

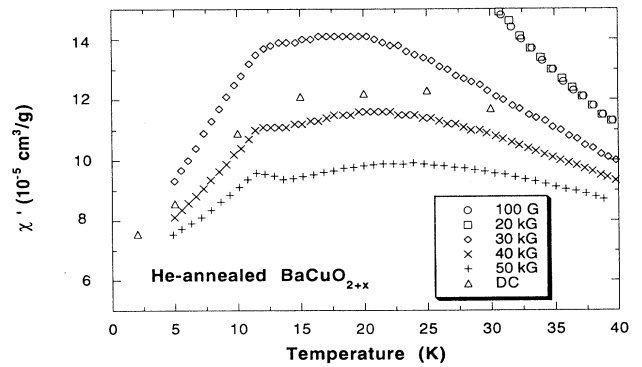

FIG. 7. Real part of the ac magnetic susceptibility χ' in various static magnetic fields vs temperature. The triangles are the high-field differential susceptibility data $\chi_0(T)$ reproduced from Fig. 5(b).

K, as shown in Fig. 5(b), suggesting the onset of long-range AF order below $T_N \sim 15$–25 K. A higher-resolution measurement of $M(T)$ at fixed $H = 55$ kG is shown in Fig. 6. The data show a clear slope change at $T_N = 12 \pm 2$ K.

The ac susceptibility for the He-annealed sample was measured at various static applied magnetic fields H, as shown in Fig. 7. The AF transition postulated above becomes very clear for $H \geq 40$ kG. The data in Figs. 5(b), 6, and 7 together suggest that some of the Cu spins in $BaCuO_{2+x}$ order antiferromagnetically at $T_N \simeq 15$ K, and the remainder remain paramagnetic down to 2 K.

IV. DETAILED ANALYSIS AND MODELING

A. Magnetization versus magnetic field and temperature for $T \ll T_N$

From Fig. 5(a), the $M(H)$ data at the lowest temperatures contain a component that saturates by $H \sim 20$ kG, and a component with magnetization proportional to H. We parametrize the high-field linear behavior as follows:

$$M(H) = M_0 + \chi_0 H \ . \tag{3}$$

By subtracting the fitted $\chi_0 H$ from the observed $M(H)$, we can examine the field dependence of the saturating contribution, normalized to the highest-field value, as shown in Fig. 8 for the data in Fig. 5(a) at 2 K, where $M_0 \equiv [M - \chi_0 H](2\text{ K}, 55\text{ kG}) = 31\mu_B$/unit cell. Also plotted are Brillouin functions $B_S(H,T)$ for $g = 2$, $T = 2$ K, and spins $S = 6$, 9, and 15. A comparison of the shapes of these Brillouin functions with the data shows that the saturation arises from a large spin $S \sim 9$. The only candidate in the structure that could have about this spin value is the Cu_{18} sphere cluster, which we therefore conclude remains paramagnetic to 2 K with a ground state

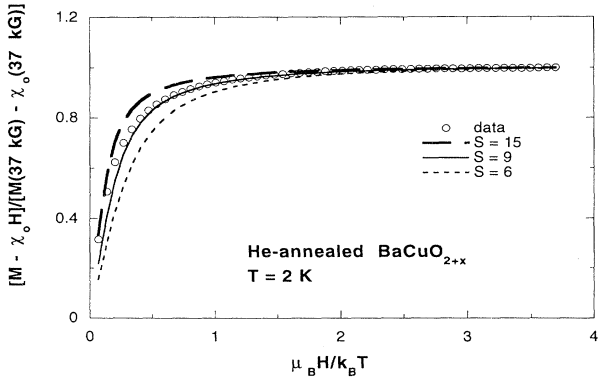

FIG. 8. The saturating part $M(H) - \chi_0 H$ of the magnetization $M(H)$ at 2 K for He-annealed $BaCuO_{2+x}$, from Fig. 5(a), normalized to $M(H = 37\text{ kG}) - \chi_0$ (37 kG), open circles, plotted vs reduced magnetic field $\mu_B H/k_B T$. Brillouin functions $B_S(H, T = 2\text{ K})$ with $g = 2$ and spins $S = 6$, 9, and 15 are also plotted vs reduced field.

with maximal spin $S_s = 18(1/2) = 9$. The Cu_6 rings thus apparently do not contribute to the saturation, and their contribution to $M(H)$ must therefore be contained in the $\chi_0 H$ term in Eq. (3). As discussed in Ref. 20, the Curie constant expected from Eq. (2) for the low-field Curie-Weiss-law susceptibility of the Cu_{18} clusters with $g = 2.1$ (from above) is $C = 49.6$ cm^3 K/(mol Cu_{18} clusters) $= 1.10$ cm^3 K/(mol Cu in $BaCuO_{2+x}$). This value is in close agreement with the value 1.13 cm^3 K/(mol Cu in $BaCuO_{2+x}$) observed between 2 and 6 K in Fig. 4, confirming that the Cu_{18} sphere clusters are primarily responsible for the Curie-Weiss susceptibility observed in Fig. 4 between 2 and 6 K, and that the Cu_6 clusters do not contribute to the Curie-Weiss susceptibility in this T range. The Weiss temperature $\theta = +0.4$ K found from Fig. 4 in this T range suggests that the Cu_{18} sphere clusters should undergo long-range ferromagnetic intercluster order at $\lesssim 1$ K.

On the other hand, the above value of $M_0(2\text{ K}) = 31\mu_B$/unit cell is about $6\mu_B$/unit cell less than the value $M_0 = 2gS_s\mu_B$/unit cell $= 37\mu_B$/unit cell expected for the two Cu_{18} clusters per unit cell, again using $g = 2.1$. The six lone Cu ions between the sphere clusters in the unit cell, located at (0.433,0,0), (0.567,0,0) and their equivalent positions in space group $Im\bar{3}m$, which are half occupied (randomly), would have a saturation moment of $6gS_{Cu}\mu_B$/unit cell $\approx 6\mu_B$/unit cell. Therefore, an average of three lone Cu ions are apparently antiferromagnetically coupled to each of the two Cu_{18} clusters in the unit cell, and their moments oppose that of the Cu_{18} cluster at low T and H. Since the magnetic behaviors of the Cu_{18} clusters and the lone Cu ions are now accounted for, the AF ordering inferred above to occur below ~ 15 K from Figs. 5(b), 6, and 7 must be due to the Cu_6 ring clusters, which are the only remaining magnetic species in the unit cell.

To summarize the above discussion, our model thus far for the magnetic properties of $BaCuO_{2+x}$ consists of the following. All of the Cu ions have an oxidation state of +2 and have spin $S_{Cu} = 1/2$. Each Cu_{18} sphere cluster has a maximal spin ground state with spin $S_s = 9$, with lower spin excited states. This ground state is consistent with the ferromagnetic nature of the nearest-neighbor Cu-Cu exchange coupling within each cluster expected from the nearly 90° Cu-O-Cu bond angle, as noted in the Introduction. For the same reason, we also expect each Cu_6 ring cluster to have a maximal spin ground state with spin $S_r = 3$. From Fig. 4, both the Cu_6 and Cu_{18} clusters are in their ground states below ~ 40 K. Below $T_N \sim 15$ K, the ground-state magnetic moments of the Cu_6 ring clusters with spins $S_r = 3$ order antiferromagnetically with respect to each other. The magnetic moments of the lone copper ions with spins $S_I = 1/2$ and of the Cu_{18} sphere clusters with spins $S_s = 9$ do not participate in this AF ordering; these species remain paramagnetic down to our low-temperature measurement limit of 2 K. The spin of each Cu_{18} sphere cluster is antiferromagnetically coupled to those of three lone Cu ions; the spin of each lone Cu ion is antiferromagnetically coupled to that of one Cu_{18} sphere cluster. The gyromagnetic factor g of the Cu_{18} sphere clusters and the lone Cu ions are both

close to 2, and a similar value is expected for the Cu_6 clusters. For $T \ll T_N$, the magnetization of the antiferromagnetically ordered Cu_6 ring clusters is proportional to H, and we denote the magnetization of a single ring by $M_r = \chi_r H$.

We now proceed to calculate the magnetization versus magnetic field and temperature expected at $T \ll T_N$ for $BaCuO_{2+x}$. On the basis of the above model, the measured magnetization $M(H,T)$ of a unit cell of $BaCuO_{2+x}$ at $T \ll T_N$ is the sum of the respective contributions from the six lone Cu ions, two Cu_{18} sphere clusters, and eight Cu_6 ring clusters:

$$M(H,T) = 6M_I(H,T) + 2M_s(H,T) + 8\chi_r(T)H \ , \quad (4)$$

where $M_I(H,T)$ and $M_s(H,T)$ are, respectively, the magnetizations of a single lone Cu ion and Cu_{18} sphere cluster. The AF coupling between M_s and M_I is taken into account using molecular field theory. The effective magnetic fields $H_{\rm eff}$ seen by $M_I(H,T)$ and $M_s(H,T)$ are then, respectively,

$$H_{{\rm eff},I} = H - \lambda M_s$$

and (5)

$$H_{{\rm eff},s} = H - 3\lambda M_I$$

where H is the applied magnetic field and $\lambda > 0$ is the antiferromagnetic molecular-field coupling constant between M_I and M_s. In the molecular-field approximation, these magnetizations are given by

$$M_x(H,T) = gS_x\mu_B B_{S_x}(H_{{\rm eff},x},T) \ , \quad (6)$$

where $x \equiv I,s$, the g values of the lone Cu ion and Cu_{18} cluster ground-state spins are assumed to be the same, and $B_S(H,T)$ is the Brillouin function for spin S.

Equations (5) and (6) constitute a set of coupled nonlinear equations. We solve them using an iterative procedure with ascending orders of approximation. To zeroth-order, one has

$$H^{(0)}_{{\rm eff},I} = H^{(0)}_{{\rm eff},s} = H \quad (7)$$

and

$$M^{(0)}_x(H,T) = gS_x\mu_B B_{S_x}(H,T) \ . \quad (8)$$

The zeroth-order magnetizations correspond to no coupling between the lone Cu ions and the Cu_{18} clusters. To general nth order, one has

$$H^{(n)}_{{\rm eff},I} = H - \lambda g S_s \mu_B B_{S_s}(H^{(n-1)}_{{\rm eff},s},T) \ ,$$
$$H^{(n)}_{{\rm eff},s} = H - 3\lambda g S_I \mu_B B_{S_I}(H^{(n-1)}_{{\rm eff},I},T) \ , \quad (9)$$

and

$$M^{(n)}_x(H,T) = gS_x\mu_B B_{S_x}(H^{(n)}_{{\rm eff},x},T) \ . \quad (10)$$

The influence of the coupling (λ) between the lone Cu ions and the Cu_{18} clusters is taken into account with increasing accuracy as the order of iteration n increases. Equations (9) and (10) were solved numerically for $M_I(H)$ and $M_s(H)$ for H in the range 5–55 kG at $T = 2$ K for a range of values of $g \sim 2$ and $\lambda \sim 10^{23}$ cm^{-3}. By plotting $M_s^{(n)}$ and $M_I^{(n)}$ versus $(1/n)^5$, an approximately linear behavior was observed. Extrapolating to $1/n = 0$, we estimate the accuracy of the calculated $M_s^{(n)}$ and $M_I^{(n)}$ to be 5 parts in 10^5 for 20th order at $H = 5000$ G, and better than 1 part in 10^7 above 15th order for $H = 55$ kG. The accuracy of M in second order (which was the approximation used in Ref. 20) is estimated to be 10% at $H = 5000$ G, which was the lowest field we used for the fit to $M(H)$ in Ref. 20, and to be 7 parts in 10^5 at $H = 55$ kG, with an average accuracy over this field range of better than 3%.

Using Eqs. (4), (9) and (10), we obtained a reasonably good fit to the $M(H)$ data between 5 and 55 kG at 2 K in Fig. 5(a) using $g = 2.0$, $\lambda = 1.34 \times 10^{23}$ cm^{-3} = 1.24 kG/μ_B and $\chi_r(2\ {\rm K}) = 5.86 \times 10^{-2}$ cm^3/(mol Cu_6 rings) $= 3.91 \times 10^{-3}$ cm^3/(mol Cu in $BaCuO_{2+x}$) for both second- and 20th-order approximations,[20,38] where the number of data to the number of parameters ratio was 65:3, as shown in Fig. 9. The reason that the g value required to obtain the best fit to the data above 5 kG in Fig. 9 (2.0) is slightly lower than inferred from the low-field data in Fig. 4 (2.1) is not clear. The fit of Eq. (4) to the $M(H,\ 2\ {\rm K})$ data, using the 20th-order calculation of M_s and M_I, is shown as the solid curve in Fig. 9, where the separate contributions of the Cu_6 clusters, the Cu_{18} clusters and the lone Cu ions are also shown.

The magnetizations at 2 K of a lone Cu ion M_I and a Cu_{18} sphere cluster M_s versus H in Fig. 9 can be understood as follows. The effective magnetic fields experienced by a Cu_{18} sphere cluster and a lone Cu ion are different. Below $H \sim 50$ kG, the effective field $H_{{\rm eff},s} = H - 3\lambda M_I$ seen by a sphere cluster is on the order of H because the opposing exchange field due to

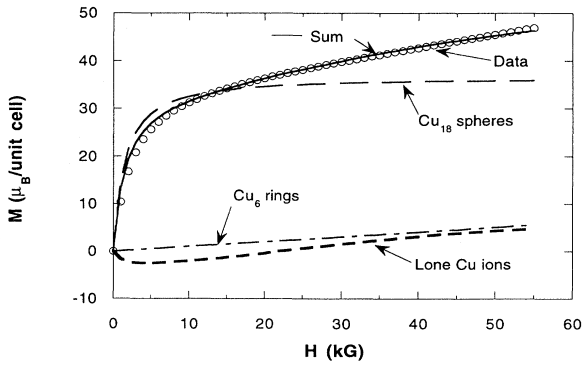

FIG. 9. Magnetization (M) vs applied magnetic field (H) for He-annealed $BaCuO_{2+x}$ at 2 K (circles) from Fig. 5(a). The solid curve labeled "Sum" is a theoretical fit to the data (see text). The contributions to the sum from the lone Cu ions, the Cu_6 ring clusters, and the Cu_{18} sphere clusters are as indicated.

AF coupling with the three neighboring lone Cu ions is relatively small compared with H. Therefore, the effective field seen by the Cu_{18} clusters is always in the direction of H. On the other hand, for H below $\sim$ 20 kG, the effective field $H_{\mathrm{eff},I} = H - \lambda M_s$ experienced by a lone Cu ion is dominated by the negative AF exchange field due to the large M_s of the sphere cluster to which the lone ion is coupled. This is the reason that M_I is initially diamagnetic in Fig. 9. When M_s becomes saturated, the exchange field $-\lambda M_s^{\max} = -22.3$ kG seen by a lone Cu ion no longer depends on H, and H can become larger than this opposing exchange field, resulting in a paramagnetic M_I, as seen in Fig. 9 above $\approx$ 20 kG. We note that to obtain the diamagnetic behavior of the lone Cu ions below 20 kG in Fig. 9, Eqs. (9) and (10) must be solved to at least second order.

The relation between the molecular-field coupling constant λ and the conventional exchange coupling constant $2J_{\mathrm{AF}}$ in the spin Hamiltonian can be estimated by going to the high-field limit, where the Brillouin function saturates to 1, and both M_I and M_s are maximally aligned with H. Then the maximum exchange field experienced by the sphere cluster is

$$H_{\mathrm{ex},s}^{\max} = -3\lambda M_I^{\max} = -3\lambda g S_I \mu_B = -3.72 \text{ kG} , \quad (11)$$

where $M_I^{\max} = gS_I\mu_B$ with $g = 2.0$ and $S_I = 1/2 = -S_{I,\max}^z$. This corresponds to exchange energy

$$\begin{aligned} E &= -\boldsymbol{M}_s^{\max} \cdot \boldsymbol{H}_{\mathrm{ex},s}^{\max} = -gS_s\mu_B H_{\mathrm{ex},s}^{\max} \\ &= 3\lambda g^2 S_I S_s \mu_B^2 = k_B(4.5 \text{ K}), \end{aligned} \quad (12)$$

where $M_s^{\max} = gS_s\mu_B$ with the same g and $S_s = 9 = -S_{s,\max}^z$. If we express this as a Heisenberg-type interaction [see Eq. (17) below]

$$E = -3(2J_{\mathrm{AF}})S_s S_I , \quad (13)$$

we get

$$2J_{\mathrm{AF}} = -\lambda g^2 \mu_B^2 = -29 \ \mu\text{eV} = k_B(-0.33 \text{ K}) . \quad (14)$$

This AF coupling between the lone Cu ions and the Cu_{18} clusters is much weaker than the FM coupling within the Cu_6 and Cu_{18} clusters (see below).

B. Low-temperature ($T \lesssim 40$ K) magnetic susceptibility

We write the magnetic susceptibility χ_{cell} of a unit cell in a manner analogous to Eq. (4):

$$\chi_{\mathrm{cell}}(T) = 6\chi_I(T) + 2\chi_s(T) + 8\chi_r(T) , \quad (15)$$

where χ_I, χ_s, and χ_r are, respectively, the susceptibilities of a lone Cu ion, a Cu_{18} sphere cluster, and a Cu_6 ring cluster. In the low-temperature range $T \lesssim 40$ K, the Cu_{18} sphere clusters are in their ground states with spin $S_s = 9$. The magnetic susceptibility χ is defined as $\chi = \lim_{H\to 0} M(H)/H$. In this low-field limit with $\mu_B H/k_B T \ll 1$, Eqs. (5) and (6) can be solved analytically[36] to yield the first two terms on the right-hand side of Eq. (15):

$$6\chi_I(T) + 2\chi_s(T) = 2\frac{(C_s + 3C_I)T - 6\lambda C_s C_I}{T^2 - 3\lambda^2 C_s C_I} , \quad (16)$$

where C_s and C_I [Eq. (2)] are, respectively, the Curie constants for a Cu_{18} sphere cluster ($S_s = 9$) and a lone Cu ion ($S_I = 1/2$). The right-hand side of Eq. (16) has the same form as for a two-sublattice ferrimagnet.[36]

Using the values $g = 2.1$ and $\lambda = 1.24$ kG/μ_B, subtraction of $6\chi_I(T) + 2\chi_s(T)$ from the observed χ yields, according to Eq. (15), the Cu_6 ring susceptibility $\chi_r(T)$. As independently deduced above in Fig. 5(b), $\chi_r(T)$ shows a maximum at $T_N \approx 13$ K, suggestive of long-range AF ordering of the Cu_6 ring cluster magnetic moments below T_N.[20] Extrapolations of the observed χ^{-1} data and predicted $[3\chi_I(T) + \chi_s(T)]^{-1}$ data indicate that the Cu_{18} sphere clusters will order ferromagnetically at a Curie temperature $T_C \lesssim 1$ K.[20] From Eqs. (2) and (16), one obtains $T_C = \lambda\sqrt{3C_I C_s} = 1.7$ K.

C. High-temperature (≥ 70 K) magnetic susceptibility

The Heisenberg model has been widely used to interpret the magnetic properties of the layered high-T_c cuprates. Similar to the Cu^{+2} ions in high-T_c cuprates, the Cu^{+2} ions in $BaCuO_{2+x}$ are spin-1/2 ions, as shown above. Therefore the exchange interaction between adjacent Cu ions should be nearly isotropic, and $BaCuO_{2+x}$ should also be well described by the Heisenberg model. The magnetic susceptibility of a cluster can be obtained, in principle, by first diagonalizing the Heisenberg Hamiltonian for the cluster,

$$\mathcal{H} = -2J\sum_{\langle i,j\rangle} \boldsymbol{S}_i \cdot \boldsymbol{S}_j , \quad (17)$$

as in the Bonner-Fisher[39] type of calculation, where in the present case $2J > 0$ is the ferromagnetic nearest-neighbor intracluster Cu-Cu superexchange coupling constant and the sum is over distinct nearest-neighbor Cu-Cu pairs within a cluster. However, due to limitations of computer memory we can only obtain the solution for up to an 11-spin cluster. Therefore we use Van Vleck's approximation[40] for the energy levels of each of the Cu_6 and Cu_{18} clusters:

$$E_{S,\alpha} = -\frac{J_\alpha z_\alpha}{n_\alpha - 1}[S(S+1) - n_\alpha S_{\mathrm{Cu}}(S_{\mathrm{Cu}}+1)] , \quad (18)$$

where $\alpha = s$ (Cu_{18} sphere cluster) or r (Cu_6 ring cluster), $n_\alpha \geq 2$ is the (even) number of Cu spins in the cluster, $S = 0,1,2, \ldots, n_\alpha S_{\mathrm{Cu}} = S_{\alpha,\max}$ is the spin of the cluster, z_α is the (average) number of nearest neighbors, and $S_{\mathrm{Cu}} = 1/2$ is the spin of a Cu^{+2} ion. Here we assume that the exchange constant J_α can be different within a sphere (J_s) and within a ring (J_r) cluster because of the different geometries of these two clusters. When the Zeeman energy $\mu_B H$ is much smaller than the thermal

energy k_BT, the susceptibility of a cluster can be written as[40]

$$\chi_\alpha(T) = \frac{N_A g^2 \mu_B^2}{3k_BT} \times \frac{\sum_{S=0}^{S=S_{\alpha,\max}} G_{S,\alpha} S(S+1)(2S+1) e^{-E_{S,\alpha}/k_BT}}{\sum_{S=0}^{S=S_{\alpha,\max}} G_{S,\alpha}(2S+1) e^{-E_{S,\alpha}/k_BT}}, \quad (19)$$

where $G_{S,\alpha}$ is the degeneracy of energy level $E_{S,\alpha}$, not counting the Zeeman degeneracy $(2S+1)$, and we assume $g_s = g_r = g$. For a cluster containing n_α spins 1/2, one has[40] $G_{S,\alpha} = \Omega(S) - \Omega(S+1)$, where $\Omega(S) = n_\alpha!/\{[(n_\alpha/2) + S]!\ [(n_\alpha/2) - S]!\}$, and $G_{S_{\alpha,\max}} = 1$.

For the sphere cluster, $n_s = 18$, $z_s = 2.667$, and $G_{S,s} = 4862$, 11 934, 13 260, 9996, 5508, 2244, 663, 135, 17, and 1 for $S = 0, 1, \ldots, 9 = S_{s,\max}$, respectively. For the ring cluster, $n_r = 6$, $z_r = 2$, and $G_{S,r} = 5, 9, 5, 1$ for $S = 0, 1, 2, 3 = S_{r,\max}$, respectively. For a lone Cu ion with spin $S_I = 1/2$, the susceptibility is taken to be a Curie Law [Eq. (1) with $\theta = 0$] denoted by $\chi_I(T)$.

The total susceptibility $\chi(T)$ of a unit cell is given again by Eq. (15). Using Eqs. (18) and (19), the expression for $1/\chi(T)$ from Eq. (15) was well fitted to our experimental data above 70 K, using $g = 2.1$, $2J_r/k_B = 290$ K and $2J_s/k_B = 80$ K, as shown in Fig. 4. These J_α parameters were obtained by minimizing the average percentage standard deviation between the calculated $\chi(T)$ and the data. The estimated standard deviation for $2J_r/k_B$ from a χ^2 analysis is 4 K and for $2J_s/k_B$ is 3 K. We also estimated in a mean-field way the effect of the antiferromagnetic interaction between the Cu_6 rings on the derived values of $2J_s$ and $2J_r$, by replacing T in the prefactor of Eq. (19) for $\chi_r(T)$ by $T - \theta$, where the effective Weiss temperature was set to be $\theta = -15\ \text{K} \sim -T_N$. This change resulted in the derived J_r and J_s values being, respectively, about 5 and 20% larger, which are within the systematic errors for $\theta = 0$ estimated below.

We have calculated the Cu_6 ring cluster magnetic energy levels exactly using a Bonner-Fisher-type[39] calculation starting from the Hamiltonian in Eq. (17) with J_r in place of J and $g = 2.1$, and the results are shown in Fig. 10(a). By computing the Cu_6 ring susceptibility $\chi_r(T)$ for various J_r values and comparing the results with those calculated using Eq. (19) and the approximate energy levels in Eq. (18), as shown in Fig. 10(b), we may estimate the systematic error in the above J_r value arising from the approximation in Eq. (18). From Fig. 10(b), we estimate that our J_r value in the above paragraph has a maximum error of ≈ 30 K, i.e., $J_r/k_B = 145 \pm 30$ K. If we assume that J_s has the same maximum percentage error, one obtains $J_s/k_B = 40 \pm 8$ K.

In the limit of high-temperatures, the exponentials in Eq. (19) can be replaced by Taylor expansions to first order in J_α/k_BT. Using the above values of n_α, z_α, and $G_{S,\alpha}$ and Eqs. (18) and (19), one obtains the susceptibilities for a single Cu_6 ring and Cu_{18} sphere cluster, given, respectively, by

$$\chi_r = \frac{g^2\mu_B^2}{3k_BT} 4.50 \left(1 + \frac{J_r}{k_BT}\right) \quad (20)$$

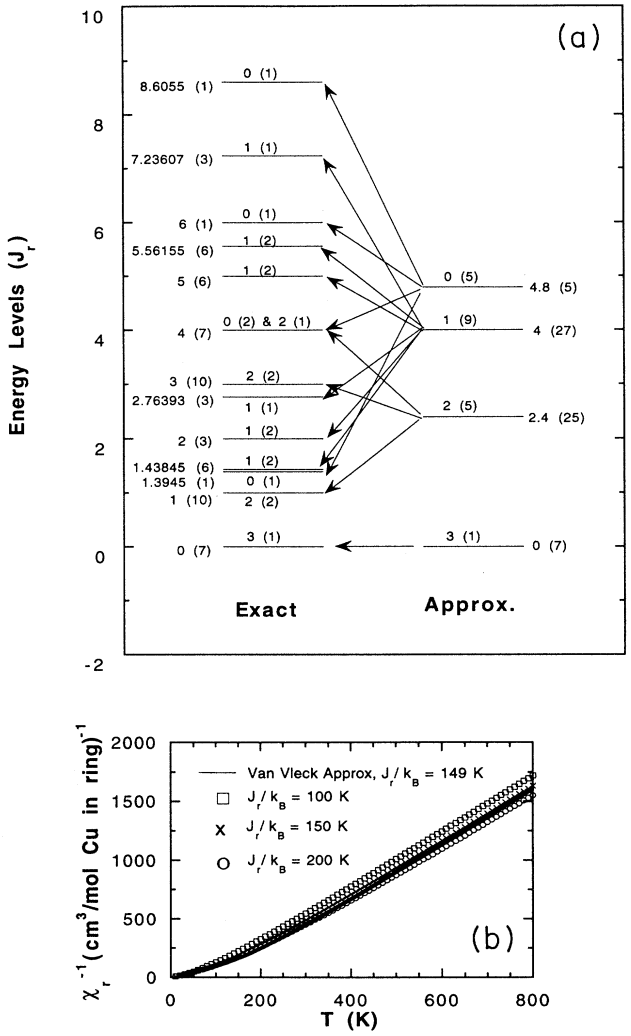

FIG. 10. (a) The energy spectrum of the eigenstates of the Heisenberg Hamiltonian, Eq. (17), for six spins 1/2 on a ring. The total degeneracies, including the Zeeman degeneracies $2S+1$, are given in parentheses beside the energy levels. The total spin S, and its degeneracy in parentheses not including the Zeeman degeneracy, are indicated near the center of the energy levels. The exact results are compared with the approximate energy levels given by Eq. (18). (b) Theoretical predictions for the inverse susceptibility χ_r^{-1} of the Cu_6 rings vs temperature. The solid curve is the prediction using Eq. (19) and the approximate cluster magnetic energy levels in Eq. (18) and in part (a) of this figure. The results of exact calculations using the Heisenberg Hamiltonian, Eq. (17), are shown by the various symbols for the corresponding values of exchange constant J_r.

and

$$\chi_s = \frac{g^2\mu_B^2}{3k_BT} 13.50 \left(1 + \frac{4J_s}{3k_BT}\right), \quad (21)$$

which contain the first correction terms in $1/T$. Using the Curie law expression for a lone Cu^{+2} ion, χ_I

$= 0.75g^2\mu_B^2/3k_BT$, the susceptibility per unit cell $\chi_{\rm cell}$ from Eqs. (15), (20), and (21) is

$$\chi_{\rm cell} = \frac{g^2\mu_B^2}{3k_BT}\left[67.5 + \frac{36(J_r + J_s)}{k_BT}\right] . \quad (22)$$

This can be written

$$\chi_{\rm cell} = \frac{C_{\rm cell}}{T - \theta} , \quad (23)$$

where the Curie constant is

$$C_{\rm cell} = \frac{N_{\rm cell}g^2 S_{\rm Cu}(S_{\rm Cu} + 1)}{3k_B} , \quad (24)$$

$N_{\rm cell} = 90$ is the number of Cu atoms/cell, $S_{\rm Cu} = 1/2$, and the Weiss temperature θ is

$$\theta = \frac{0.533(J_r + J_s)}{k_B} . \quad (25)$$

Equation (23) shows that the high-temperature susceptibility follows a Curie-Weiss law, where from Eq. (24) the Curie constant is the same as for noninteracting Cu^{+2} spins, as observed above $\sim$ 300 K in Fig. 4. The intracluster interactions manifest themselves in the existence and value of θ in Eq. (25). If the T range over which Eq. (23) is fitted to the data is not quite in the high-T limit, the measured θ would be smaller than given by Eq. (25) for the fitted values of J_r and J_s. With this consideration in mind, the value $\theta = 81$ K determined from the data above 300 K in Fig. 4 compares favorably with the value $\theta = (99 \pm 17)$ K computed from Eq. (25) using the above values of J_r and J_s.

V. SUMMARY AND CONCLUSIONS

The compound $BaCuO_{2+x}$ ($x \sim 0$) is a unique cuprate with a large cubic unit cell ($a_0 = 18.3$ Å) containing 90 formula units. The cell contains six lone Cu ions, two Cu_{18} sphere clusters, and eight Cu_6 ring clusters. In this paper, we have described in detail the results of static magnetization and ac magnetic susceptibility measurements of $BaCuO_{2+x}$ ($x \approx 0.1$) and a model to self-consistently explain the magnetic properties, summaries of some of which were given in Ref. 20. It is remarkable that despite its complexity, the spin system can be adequately described by a simple cluster model, where the populations of the internal magnetic energy levels of the clusters are temperature dependent.

At high-temperatures $T \geq 300$ K, the static susceptibility χ exhibits a Curie-Weiss temperature dependence with a ferromagnetic (FM) Weiss temperature $\theta = 81$ K, and with an effective moment $\mu_{\rm eff} = 1.82\mu_B$/Cu atom, which is essentially identical with the Cu^{+2} spin-only value. On the basis of these data alone, one infers that all of the Cu species are Cu^{+2} with spin $S_{\rm Cu} = 1/2$. Mean-field theory predicts that long-range FM ordering of these spins should occur at a Curie temperature $T_C = \theta$. In contrast, $\chi^{-1}(T)$ is found to exhibit positive curvature with decreasing T, and approaches a Curie law ($\theta \approx 0$) as $T \to 0$ with a much larger (average) effective moment per Cu ion than at high T, confirming an earlier report.[28] Static magnetization measurements and differential ac susceptibility measurements at high (30–55 kG) magnetic field indicated the occurrence of an antiferromagnetic rather than a FM transition at $T_N \sim 12$ K, consistent with previous ESR (Ref. 28) and neutron diffraction (Ref. 31) data, although no distinct feature was observed at T_N in the (low-field) $\chi(T)$ data.

Crucial information unifying the above observations was obtained from a magnetization-versus-field isotherm at 2 K. These data, together with the $\chi(T)$ data, showed that (i) remarkably, the lone Cu ions and the Cu_{18} clusters do not participate in the magnetic ordering at $\sim$ 15 K and therefore that the ordering must arise from the Cu_6 clusters only; (ii) the Cu_{18} sphere clusters have a FM ground state with maximal spin $S_s = 9$; (iii) the Cu_{18} clusters are antiferromagnetically coupled to the lone Cu ions (spin $S_I = 1/2$) with superexchange coupling constant $2J_{\rm AF}/k_B = -0.33$ K; and (iv) the Cu_{18} clusters should exhibit ferromagnetic intercluster ordering below $\sim$ 1 K. From the similarity of the internal geometries of the Cu_6 and Cu_{18} clusters, we inferred that (v) the Cu_6 ring clusters should also have a FM ground state with maximal spin $S_r = 3$. From the $\chi(T)$ data, the two types of clusters appear to be in their ground states below $\sim$ 40 K $\gg T_N$. The lack of a distinct feature in the $\chi(T)$ data at T_N occurs because the nearly Curie-law temperature dependence of χ at low T, arising mainly from the paramagnetic Cu_{18} clusters, overwhelms the opposite T dependence below T_N expected from AF ordering of the Cu_6 ring clusters. Features (i) and (v) have been confirmed by magnetic neutron diffraction measurements.[20,32] The FM coupling within the clusters is attributed to the nearly 90° bond angle of the Cu-O-Cu superexchange pathway. By contrast, the 180° bond angle found in the layered high-superconducting transition-temperature cuprates results in the well-known strong ($2J \approx -1500$ K) AF superexchange coupling.[3,5] Since the 90° superexchange coupling in $BaCuO_{2+x}$ is of higher perturbation order than the 180° coupling in the layered cuprates, the magnitude of the 90° superexchange coupling is expected, and found here, to be smaller than that of the 180° coupling.

The decrease in the (average) effective moment per Cu ion with increasing temperature arises because the excited states of the Cu_6 and Cu_{18} clusters, which have lower spins than the ground states, become populated with increasing T, thereby reducing the susceptibility from that extrapolated from low T. This scenario was confirmed by the excellent fit of theory to the $\chi(T)$ data from 70 to 400 K, which also yielded the FM intracluster superexchange coupling constants $2J_s = (80 \pm 16)$ K and $2J_r = (290 \pm 60)$ K for the sphere and ring clusters, respectively. The Cu^{+2} positions in the sphere clusters, unlike those in the ring clusters, are not all equivalent; AF contributions at high symmetry sites of the sphere clusters may be present and lead to the lower (average) value of $2J_s$ relative to the $2J_r$ inferred for the ring clusters. In the limit of high T, one expects a Curie-Weiss

temperature dependence of $\chi(T)$ with a θ reflecting the sign and magnitudes of J_r and J_s, and with a molar Curie constant C which is the same as for uncoupled Cu^{+2} ions. The reason that C is the same as for uncoupled Cu^{+2} ions at high T is that the high T corrections to the C for the uncoupled ions depend on the ratios of the exchange to thermal energies J_α/k_BT, which become small at high T. Thus, at high T and for a mole of $BaCuO_{2+x}$, from Eq. (2) one obtains

$$C = \frac{N_A g^2 (1/2)(3/2)}{3k_B} = 0.75 \frac{N_A g^2}{3k_B} . \quad (26)$$

When the clusters are in their ground states (below $\sim$ 40 K), and in the absence of AF ordering of the ring clusters, one would obtain

$$C = \frac{N_A g^2}{3k_B} \frac{6S_I(S_I+1) + 8S_r(S_r+1) + 2S_s(S_s+1)}{90} = 3.12 \frac{N_A g^2}{3k_B} , \quad (27)$$

where $S_I = 1/2$, $S_r = 3$, and $S_s = 9$. Comparison of Eqs. (26) and (27) shows that the Curie constant for the same total number of Cu^{+2} ions is much greater at low T when the clusters are in their ground states than at high T when all spin states $S = 0, 1, \ldots, S_{\alpha,\max}$ within each cluster are nearly equally populated. This difference in Curie constants is primarily responsible for the positive curvature in $\chi^{-1}(T)$ in Fig. 4 below $\sim$300 K. A similar $\chi^{-1}(T)$ behavior was found for a ferromagnetically coupled Cr_4 cluster, which has a spin 6 ground state and spin 5,4,...,0 excited states.[37]

In view of the above model for the magnetic properties of $BaCuO_{2+x}$, we speculate that the ESR signal observed for this compound[28,29] arises from the lone Cu^{+2} ions which in turn probe their magnetic environment. The g-value and linewidth-versus-temperature data reported in Ref. 28 exhibit, in addition to an anomaly associated with the AF transition at $T_N = 13$ K, a second but more subtle anomaly at $T \sim 40$ K. Since in our model a lone Cu ion is weakly exchange coupled to its nearest-neighbor Cu_{18} sphere cluster, the 40 K anomaly may be associated with the internal FM ordering within these clusters with decreasing T, whereas the anomaly at 13 K occurs because of the local magnetic dipolar field at a lone Cu site from the Cu_6 ring clusters, which order at $T_N \sim 13$ K. Detailed analysis of such ESR results within the context of the present model should be able to test these speculations.

In the field of high-temperature superconductivity, the conditions under which the Cu-O-Cu superexchange coupling is either ferromagnetic or antiferromagnetic are of prime importance. The present work provides a clear demonstration of ferromagnetic Cu-O-Cu superexchange coupling within the Cu_6 and Cu_{18} clusters in $BaCuO_{2+x}$. This compound is one of very few cuprates in which such ferromagnetic superexchange has been proven to occur. Extension of the present studies to isostructural $BaNiO_{2+x}$ compounds[41] and $Ba(Cu_{1-y}Ni_y)O_{2+x}$ solid solutions would be very interesting.

ACKNOWLEDGMENTS

We would like to thank H. Takeya, J. Moorman, and K. A. Gschneidner, Jr. for help in measuring ac susceptibility, K. M. Ho and C. T. Chan for use of their computer workstation, and X.-L. Wang and J. A. Fernandez-Baca for stimulating discussions. Ames Laboratory is operated for the U.S. Department of Energy by Iowa State University under Contract No. W-7405-Eng-82. This work was supported by the Director for Energy Research, Office of Basic Energy Sciences.

[1] *Chemistry of Superconductor Materials*, edited by T. A. Vanderah (Noyes, Park Ridge, NJ, 1992).
[2] D. Vaknin, S. K. Sinha, D. E. Moncton, D. C. Johnston, J. M. Newsam, C. R. Safinya, and H. E. King, Jr., Phys. Rev. Lett. **58**, 2802 (1987).
[3] For a review, see D. C. Johnston, J. Magn. Magn. Mater. **100**, 218 (1991).
[4] G. Shirane, R. J. Birgeneau, Y. Endoh, P. Gehring, M. A. Kastner, K. Kitazawa, H. Kojima, I. Tanaka, T. R. Thurston, and K. Yamada, Phys. Rev. Lett. **63**, 330 (1989).
[5] For a review, see R. J. Birgeneau and G. Shirane, in *Physical Properties of High Temperature Superconductors I*, edited by D. M. Ginsberg (World Scientific, Singapore, 1989), p. 151.
[6] G. Shirane, Y. Endoh, R. J. Birgeneau, M. A. Kastner, Y. Hidaka, M. Oda, M. Suzuki, and T. Murakami, Phys. Rev. Lett. **59**, 1613 (1991).
[7] P. W. Anderson, Science **235**, 1196 (1987); J. R. Schrieffer, X.-G. Wen, and S.-C. Zhang, Phys. Rev. Lett. **60**, 944 (1988); D. J. Scalapino, J. Phys. Chem. Solids **54**, 10 (1993); P. Monthoux and D. Pines, Phys. Rev. B **49**, 4261 (1994).
[8] P. W. Anderson, Phys. Rev. **79**, 350 (1950).
[9] J. B. Goodenough, *Magnetism and the Chemical Bond* (Interscience, New York, 1963).
[10] A. Aharony, R. J. Birgeneau, A. Coniglio, M. A. Kastner, and H. E. Stanley, Phys. Rev. Lett. **60**, 1330 (1988).
[11] D. Klemm, M. Letz, E. Sigmund, and G. S. Zavt, Phys. Rev. B **50**, 7046 (1994), and references cited.
[12] B. Büchner, M. Breuer, A. Freimuth, and A. P. Kampf, Phys. Rev. Lett. **73**, 1841 (1994).
[13] F. Mizuno, H. Masuda, I. Hirabayashi, S. Tanaka, M. Hasegawa, and U. Mizutani, Nature (London) **345**, 788 (1990); H. Masuda, F. Mizuno, I. Hirabayashi, and S. Tanaka, Phys. Rev. B **43**, 7871 (1991).
[14] F. Sapiña, J. Rodriguez-Carvajal, M. J. Sanchis, R. Ibáñez, A. Beltrán, and D. Beltrán, Solid State Commun. **74**, 779 (1990).
[15] K. Seedhar and P. Ganguly, Inorg. Chem. **27**, 2261 (1988).
[16] K. Okuda, S. Noguchi, K. Konishi, H. Deguchi, and K.

Takeda, J. Magn. Magn. Mater. **104-107**, 817 (1992).
[17] R. Hoffman, R. Hoppe, and W. Schäfer, Z. Anorg. Allg. Chem. **578**, 18 (1989).
[18] R. Kipka and Hk. Müller-Buschbaum, Z. Naturforsh. Teil B **32**, 121 (1977); for a review, see Hk. Müller-Buschbaum, Angew. Chem. Int. Ed. Engl. **16**, 674 (1977).
[19] M. T. Weller and D. R. Lines, J. Solid State Chem. **82**, 21 (1989).
[20] Z.-R. Wang, X.-L. Wang, J. A. Fernandez-Baca, D. C. Johnston, and D. Vaknin, Science **264**, 402 (1994). In this paper the λ values were quoted as 10 and 9.5, respectively. The units of λ, $(N_A/45)$ cm^{-3}, were inadvertantly omitted. The quoted value for J_{AF} (1.3 meV) is incorrect. The correct value, $2J_{AF} = -29$ μeV, is given here in Eq. (14). The units on the left ordinate of Fig. 2(b) are mislabeled by a factor of 10. The correct units are 10^{-3} cm^3/mol of Cu in $BaCuO_{2+x}$.
[21] E. F. Paulus, G. Miehe, H. Fuess, I. Yehia, and U. Lochner, J. Solid State Chem. **90**, 17 (1991).
[22] S. Eriksson, L. Johansson, L. Borjesson, and M. Kakihana, Physica C **162-164**, 59 (1989).
[23] For a review, see W. Wong-Ng and R. S. Roth, Powder Diffract. **9**, 280 (1994).
[24] M. A. G. Aranda and J. P. Attfield, Angew. Chem. Int. Ed. Engl. **32**, 1454 (1993).
[25] D. Eckert, A. Junod, T. Graf, and J. Muller, Physica C **153**, 1038 (1988); for a review, see R. A. Fisher, J. E. Gordon, and N. E. Phillips, J. Supercond. **1**, 231 (1988).
[26] H. N. Migeon, F. Jeannot, M. Zanne, and J. Aubry, Rev. Chim. Min. **13**, 440 (1976); H. N. Migeon, M. Zanne, F. Jeannot, and C. Gleitzer, *ibid.* **14**, 498 (1977).
[27] M. Wu, Q. Su, G. Hu, Y. Ren, and H. Wang, J. Solid State Chem. **110**, 389 (1994).
[28] D. C. Vier, S. B. Oseroff, C. T. Salling, J. F. Smyth, S. Schultz, Y. Dalichouch, B. W. Lee, M. B. Maple, Z. Fisk, and J. D. Thompson, Phys. Rev. B **36**, 8888 (1987).
[29] R. N. de Mesquita, J. H. Castilho, G. E. Barberis, C. Rettori, I. Torriani, M. C. Terrile, H. Basso, and O. R. Nascimento, Phys. Rev. B **39**, 6694 (1989).
[30] S. Petricek, N. Bukovec, and P. Bukovec, J. Solid State Chem. **99**, 58 (1992).
[31] D. Vaknin (unpublished).
[32] X.-L. Wang, J. A. Fernandez-Baca, Z. R. Wang, D. Vaknin, and D. C. Johnston, Physica B (to be published).
[33] X.-L. Wang, J. A. Fernandez-Baca, Z. R. Wang, D. Vaknin, and D. C. Johnston (unpublished).
[34] P. W. Selwood, *Magnetochemistry*, 2nd ed. (Interscience, New York, 1956), p. 78.
[35] D. C. Johnston, T. Matsumoto, Y. Yamaguchi, Y. Hidaka, and T. Morakami, in *Electronic Properties and Mechanisms of High Temperature Superconductors*, edited by T. Oguchi, K. Kadowaki, and T. Sasaki (Elsevier, Amsterdam, 1992), p. 301.
[36] C. Kittel, *Introduction to Solid State Physics*, 6th ed. (Wiley, New York, 1986).
[37] A. Bino, D. C. Johnston, D. P. Goshorn, T. R. Halbert, and E. I. Stiefel, Science **241**, 1479 (1988).
[38] Conventionally, one writes $H_{eff} = H - \lambda' M$, where M is the volume magnetization and λ' is dimensionless. In terms of our λ, the conventional λ' is given by $\lambda' = \lambda(V_{cell}/2)$, where $V_{cell} = 6.12 \times 10^{-21}$ cm^3 is the unit cell volume. Thus, for $\lambda = 1.34 \times 10^{23}$ cm^{-3}, one obtains $\lambda' = 410$.
[39] J. C. Bonner and M. E. Fisher, Phys. Rev. **135**, A640 (1964).
[40] J. H. Van Vleck, *The Theory of Electric and Magnetic Susceptibilities* (Oxford University Press, London, 1965).
[41] R. Gottschall and R. Schöllhorn, Solid State Ionics **59**, 93 (1993).